

CHARACTERIZATION OF ELECTRONIC WASTE MATERIALS BY INSTRUMENTAL NEUTRON ACTIVATION ANALYSIS FOR CERTIFIED REFERENCE MATERIAL PRODUCTION

M. Di Luzio¹/Presenter, L. Bergamaschi², R. Jacimovic³, G. D'Agostino⁴

¹ Istituto Nazionale di Ricerca Metrologica (INRIM), Pavia, Italy, m.diluzio@inrim.it

² Istituto Nazionale di Ricerca Metrologica (INRIM), Pavia, Italy, l.bergamaschi@inrim.it

³ Jozef Stefan Institute (JSI), Ljubljana, Slovenia, radojko.jacimovic@ijs.si

⁴ Istituto Nazionale di Ricerca Metrologica (INRIM), Pavia, Italy, g.dagostino@inrim.it

Abstract:

Recycling of Waste from Electrical and Electronic Equipment provides an accessible source to gather Technology Critical Elements which are in constant need. The main metrological challenge consists in the lack of Certified Reference Materials for this kind of matrices impeding to perform SI traceable and reliable analytical measurements on those heterogeneous materials.

This work describes the adoption of relative- and k_0 -standardization of Instrumental Neutron Activation Analysis to quantify some of the Technology Critical Elements for certification in two Reference Material candidates.

Keywords: WEEE; INAA; Reference Material

1. INTRODUCTION

Electronic devices are ubiquitous within the European Union and their ever increasing demand is putting a lot of pressure on the supply chain, especially for what concerns materials defined as Technology Critical Elements (TCE). Waste from Electrical and Electronic Equipment (WEEE) can provide an accessible source to gather TCE; to this end, the European Union highly encourages practices involving more sensible waste management aiming to recycle those elements. However, a primary metrological obstacle to the recycling lies in the lack of Certified Reference Material (CRM) for this heterogeneous compound which makes difficult to perform SI traceable and reliable analytical measurements on waste samples.

Within the European project MetroCycleEU, samples from two WEEE materials from end-of-life Printed Circuit Boards (PCB) and Light-Emitting Diodes (LED) were prepared and characterized to be evaluated as candidates with the aim to produce the corresponding CRMs. The maximum allowed target standard uncertainty ($k = 1$) for the certified

TCE mass fractions was fixed to 20%, including inhomogeneity and value assignment.

In detail, gathered materials were grinded to powder and analyzed by different analytical techniques to quantify interesting TCE present with mass fraction greater than $1 \mu\text{g g}^{-1}$.

In this work the adoption of relative- and k_0 -standardization of Instrumental Neutron Activation Analysis (INAA) to quantify TCE in samples of candidate CRMs is described. INAA provides suitable reference methods for bulk analysis preventing the dissolution of sample which is usually a challenging task for highly heterogeneous materials. The optimized INAA measurement procedures are reported and results for quantified TCE in both matrices are plotted on a sample-per-sample basis; major contributors to uncertainties are identified based on the provided uncertainty budgets, which also support SI traceability.

2. MEASUREMENT MODELS

INAA is an elemental analytical technique based on excitation of samples with a neutron flux and subsequent detection of γ -emissions from the produced radionuclides [1]. Since neutrons and γ -rays have great penetration in matter, the technique is suitable for bulk analysis and allows to limit or completely avoid sample preparation.

The two main standardization methods adopted with INAA are referred to as (i) relative [2] and (ii) k_0 [3]; while the basic concept of the technique remains the same they differ about the standardization element used for analysis. In the relative method a standard, containing the same element to be quantified, is co-irradiated with the measurement sample whereas in the k_0 method the co-irradiated standard contains a monitor element that is not necessarily the element to be quantified.

In the relative method a direct comparison between standard and sample is performed through the ratio of the corresponding count rate emissions.

The k_0 method instead needs the knowledge of neutron flux parameters, alongside with specific composite nuclear constants, to relate data from the analyte element to the monitor element.

A general measurement model is described, suitable for both analytical methods, to measure the mass fraction of the analyte element, w_a , in the sample:

$$w_a = \frac{C_{s a} k_{0 \text{Au}}(m)}{C_{s m} k_{0 \text{Au}}(a)} k_\varepsilon k_\beta \frac{m_{\text{std}} (1 - \eta_{\text{std}})}{m_{\text{sm}} (1 - \eta_{\text{sm}})} w_m$$

$$\times \frac{G_{\text{th m}} + \frac{G_{e m}}{f} \left(\frac{Q_{0 m} - 0.429}{\bar{E}_{r m}^\alpha} + \frac{0.429}{0.55^\alpha (2\alpha + 1)} \right)}{G_{\text{th a}} + \frac{G_{e a}}{f} \left(\frac{Q_{0 a} - 0.429}{\bar{E}_{r a}^\alpha} + \frac{0.429}{0.55^\alpha (2\alpha + 1)} \right)} \quad (1)$$

where subscript a, m, sm and std refer to the analyte element, monitor element, measurement sample and standard sample, respectively. The C_s parameter represents the count rate at saturation, $k_{0 \text{Au}}$ is the k_0 value, k_ε is the efficiency ratio between analyte and monitor, k_β is the correction due to neutron flux gradient for measurement and standard samples, G_{th} and G_e are neutron self-shielding corrections, f is the thermal to epithermal conventional flux ratio, Q_0 is the resonance integral $1/E$ to 2200 m s^{-1} cross section ratio, \bar{E}_r is the effective resonance energy, α is the deviation from the $1/E$ trend of the epithermal flux, m is the mass, η is the moisture correction and w is the mass fraction. Details of the measurement model and its validation can be found in [4] and [5], respectively.

The model reported in eq. (1) is valid either for relative and k_0 -method; however, in the first case some of the factors simplify completely or assume values close to 1 due to the adoption of the same element for analyte and monitor: this situation applies for $\frac{k_{0 \text{Au}}(m)}{k_{0 \text{Au}}(a)}$ and to some extent, k_ε and

$$\frac{G_{\text{th m}} + \frac{G_{e m}}{f} \left(\frac{Q_{0 m} - 0.429}{\bar{E}_{r m}^\alpha} + \frac{0.429}{0.55^\alpha (2\alpha + 1)} \right)}{G_{\text{th a}} + \frac{G_{e a}}{f} \left(\frac{Q_{0 a} - 0.429}{\bar{E}_{r a}^\alpha} + \frac{0.429}{0.55^\alpha (2\alpha + 1)} \right)}. \text{ Accordingly, the}$$

combined uncertainty obtained via the relative method is expected to be lower with respect to a similar measurement performed with the k_0 method as long as the uncertainty on counting statistics is comparable and under control; the usual higher uncertainty of the k_0 method is due to the corrections needed for the analyte to monitor conversion which depend on results of detector and irradiation facility characterizations and literature values [6], all parameters that have little to no impact on the relative method.

3. EXPERIMENTAL

Materials recovered from WEEE and available within the MetroCycleEU project were measured to evaluate their suitability as candidate CRMs. Test batches obtained from end-of-life PCB and LED milled to a particle size below $200 \mu\text{m}$ were shipped to the Jozef Stefan Institute (JSI) and Istituto Nazionale di Ricerca Metrologica (INRIM) laboratories to perform INAA quantification of the critical elements Au, Co, La and Ta. The k_0 -standardization was adopted by JSI and the relative-standardization was adopted by INRIM, respectively.

3.1. Printed Circuit Boards (PCB)

From the batch of PCB material delivered to JSI, 8 measurement samples (4 of about 0.20 g and 4 of about 0.30 g) were sealed into pure polyethylene ampoules while moisture content was assessed on a separated aliquot. For determination of short-lived radionuclides, 4 samples and corresponding Al-0.1%Au standards (ERM-EB530A alloy) were stacked together, fixed in polyethylene vial and irradiated for 30 seconds in the carousel facility (CF) of the TRIGA Mark II reactor with a thermal neutron flux of $1.1 \times 10^{12} \text{ cm}^{-2} \text{ s}^{-1}$. For determination of intermediate and long-lived radionuclides, 4 samples and corresponding Al-0.1%Au standards were prepared on the same way as above and irradiated for 1 hour in the CF of the TRIGA Mark II reactor. After short irradiation (30 seconds) samples were measured after 15, 25, 120 minutes, 24 hours and 15 days of cooling time on absolutely calibrated HPGe detectors (40% and 45 % relative efficiency). After long irradiation (1 hour) samples were measured after 4, 11 and 30 days of cooling time on the same detectors. For peak area evaluation, the HyperLab program was used. The values $f = 22.54$ and $\alpha = -0.0075$, obtained from previous determinations using the Cd ratio method, were adopted as flux parameters.

From the batch of PCB material delivered to INRIM, 12 measurement samples of about 0.17 g each were prepared while moisture content was assessed on a separate aliquot by means of a thermo-balance. Standard samples were prepared by pipetting drops of Au, Co, La and Ta SI-traceable solutions; measurement and standard samples were stacked in 3 irradiation containers and irradiated in the CF of TRIGA Mark II reactor of Pavia with a thermal neutron flux of $1.2 \times 10^{12} \text{ cm}^{-2} \text{ s}^{-1}$; the irradiation lasted 1 h with the reactor operating at 250 kW power. Spectra of measurement and standard samples were acquired at suitable counting positions (ranging from 200 mm to 20 mm) of a 50 % relative efficiency HPGe detector.

3.2. Light Emitting Diodes (LED)

From the batch of LED material delivered to JSI, 12 measurement samples (5 for short irradiation and 7 for long irradiation) of about 0.25 g each were sealed into pure polyethylene ampoules. The same procedure as mentioned above for PCB was applied, except for the long irradiation duration, which lasted 12 hours.

From the batch of LED material delivered to INRIM, 16 measurement samples of about 0.40 g each were prepared while moisture content was assessed on a separate aliquot by means of a thermo-balance. Standard samples were prepared by pipetting drops of Au, Co, La and Ta SI-traceable solutions; measurement and standard samples were stacked in 4 irradiation containers then split in two irradiations in the CF of TRIGA Mark II reactor of Pavia; the short irradiation, designed to limit the matrix activation for quantification of medium-lived nuclides (Au and La), lasted 30 min while the long irradiation, designed for quantification of long-lived nuclides (Co and Ta), lasted 3 h. Spectra of measurement and standard samples were acquired at suitable counting positions (ranging from 200 mm to 20 mm) of a 50 % and a 20 % relative efficiency HPGe detector.

4. RESULTS

Data collected in the k_0 -NAA experiment performed at JSI were elaborated with the software package Kayzero for Windows V3.40, which includes effective solid angle algorithms for detection efficiency calculations. Results are

provided with combined uncertainty considering all known contributors (k_0 -related literature values [6], irradiation, decay and measuring times, sample mass, standard composition, flux parameters, detection efficiency and related corrections).

Data collected in the relative-NAA experiment performed at INRIM were elaborated with the aid of a homemade software implementing eq. (1) to get mass fraction results of the investigated elements together with uncertainty budgets. Input parameters were provided from knowledge of the experimental setup (dimensions and content of samples, γ -counting distances, γ -peak net areas and times of the acquired spectra), previous measurements (detector efficiency characterization, flux parameters), and literature (activation and decay related parameters [6]).

As anticipated, the relative method allows reaching an uncertainty significantly lower than the k_0 -method.

4.1. Printed Circuit Boards (PCB)

Mass fraction results concerning the quantification of Au, Co, La and Ta in the PCB samples and obtained by JSI and INRIM are hereafter reported. Additionally, relative differences with respect to the average of all mass fraction results concerning the same element, \bar{w} , are also given together with indication of the contribution to the combined uncertainty, I , of the three main macro-components obtained by grouping parameters related to (i) counting statistics, (ii) detection efficiency and (iii) the remaining ones, respectively.

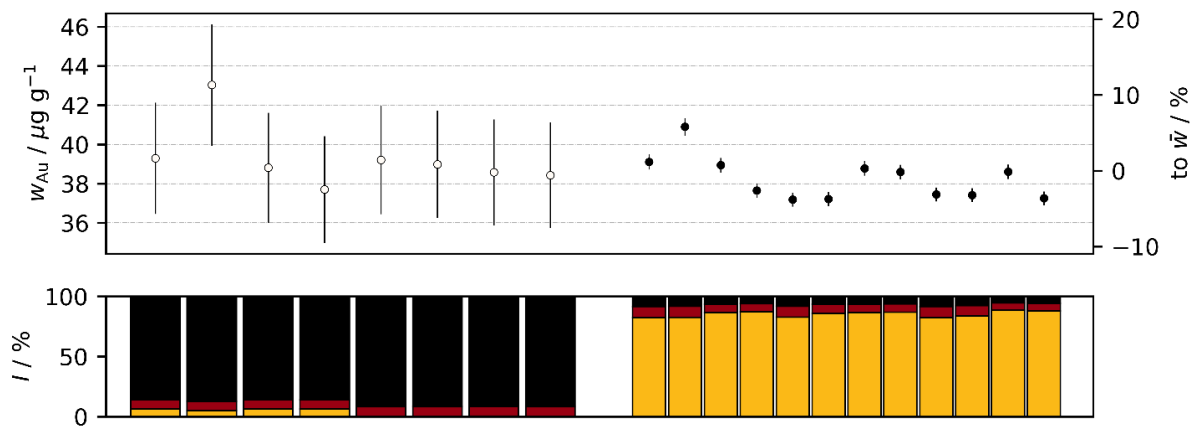


Figure 1: Au mass fractions measured on samples of the PCB material. White and black circles display results obtained with k_0 -NAA and relative-NAA, respectively; error bars indicate expanded uncertainty ($k = 2$). The bar chart at the bottom reports the contributions to the uncertainty for the corresponding value: the highlighted macro-contributors are counting statistics (yellow), efficiency (red) and the remaining ones (black).

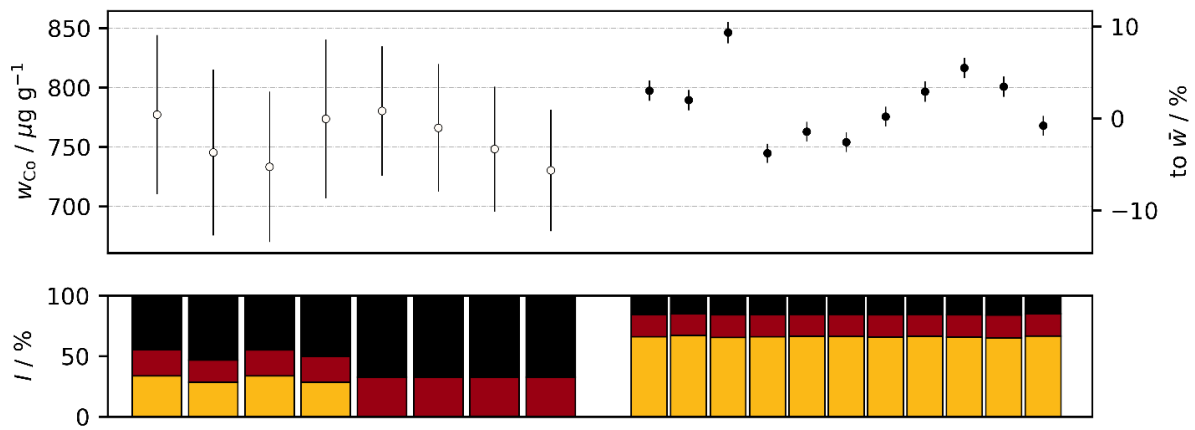


Figure 2: Co mass fractions measured on samples of the PCB material. White and black circles display results obtained with k_0 -NAA and relative-NAA, respectively; error bars indicate expanded uncertainty ($k = 2$). The bar chart at the bottom reports the contributions to the stated uncertainty for the corresponding value: the highlighted macro-contributors are counting statistics (yellow), efficiency (red) and the remaining ones (black).

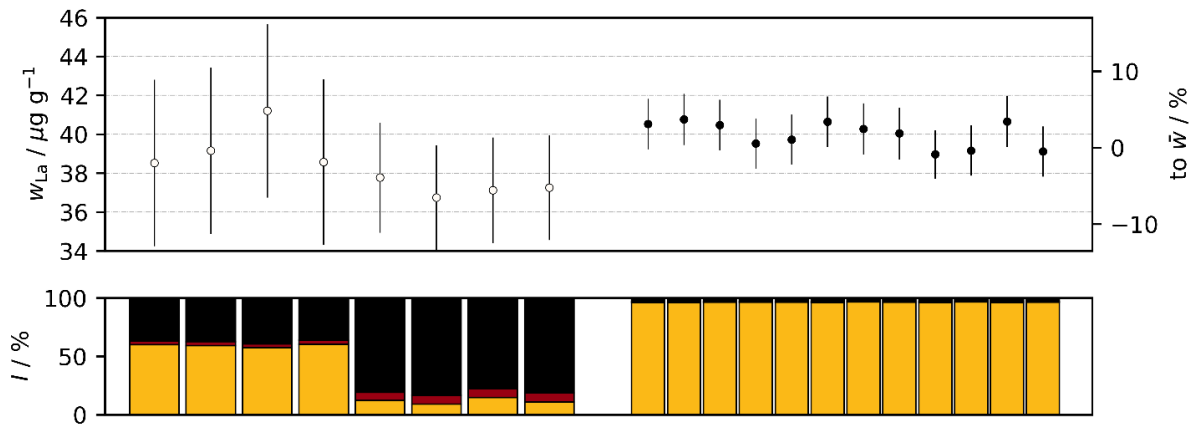


Figure 3: La mass fractions measured on samples of the PCB material. White and black circles display results obtained with k_0 -NAA and relative-NAA, respectively; error bars indicate expanded uncertainty ($k = 2$). The bar chart at the bottom reports the contributions to the stated uncertainty for the corresponding value: the highlighted macro-contributors are counting statistics (yellow), efficiency (red) and the remaining ones (black).

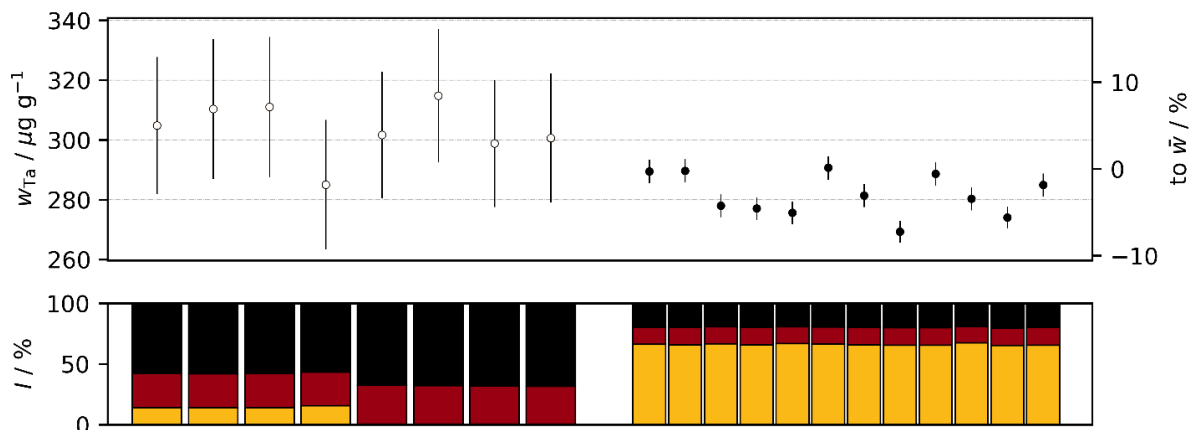


Figure 4: Ta mass fractions measured on samples of the PCB material. White and black circles display results obtained with k_0 -NAA and relative-NAA, respectively; error bars indicate expanded uncertainty ($k = 2$). The bar chart at the bottom reports the contributions to the stated uncertainty for the corresponding value: the highlighted macro-contributors are counting statistics (yellow), efficiency (red) and the remaining ones (black).

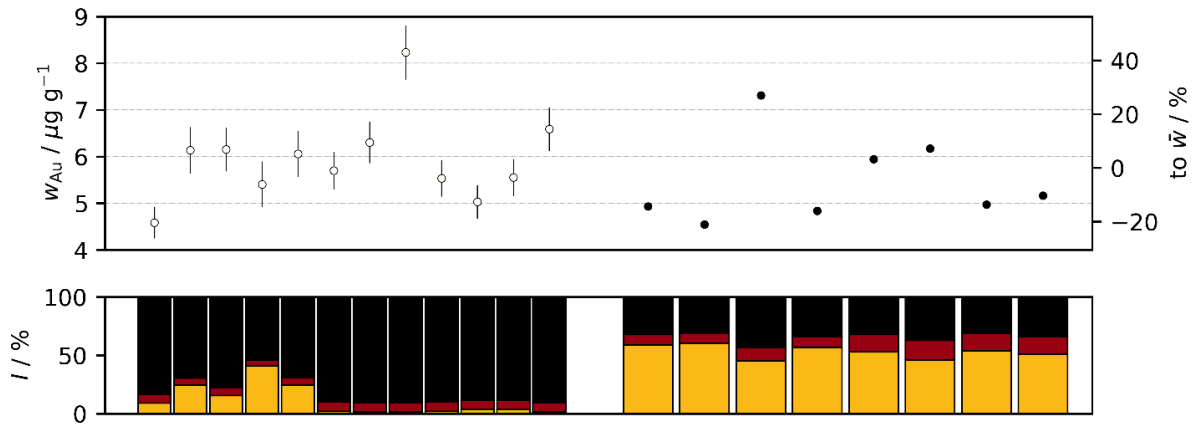


Figure 5: Au mass fractions measured on samples of the LED material. White and black circles display results obtained with k_0 -NAA and relative-NAA, respectively; error bars indicate expanded uncertainty ($k = 2$). The bar chart at the bottom reports the contributions to the stated uncertainty for the corresponding value: the highlighted macro-contributors are counting statistics (yellow), efficiency (red) and the remaining ones (black).

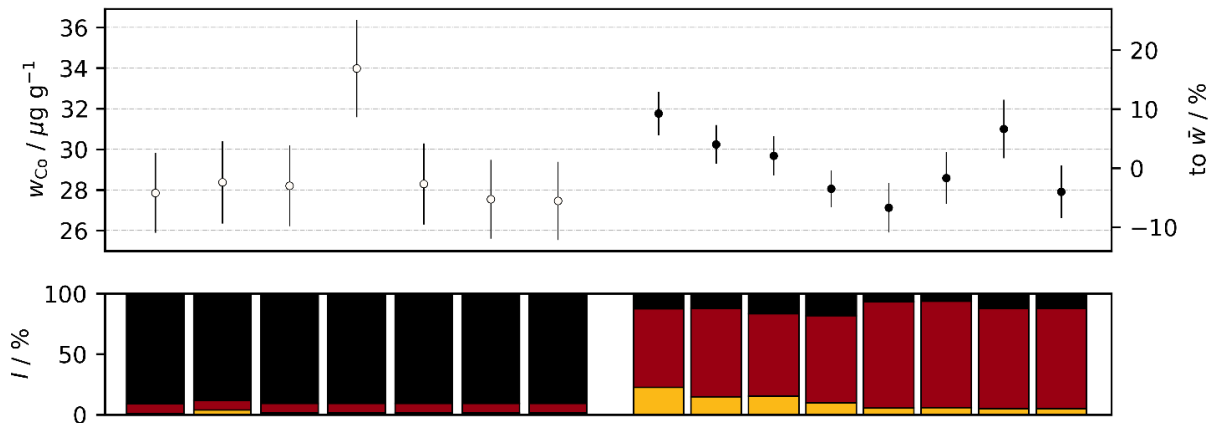


Figure 6: Co mass fractions measured on samples of the LED material. White and black circles display results obtained with k_0 -NAA and relative-NAA, respectively; error bars indicate expanded uncertainty ($k = 2$). The bar chart at the bottom reports the contributions to the stated uncertainty for the corresponding value: the highlighted macro-contributors are counting statistics (yellow), efficiency (red) and the remaining ones (black).

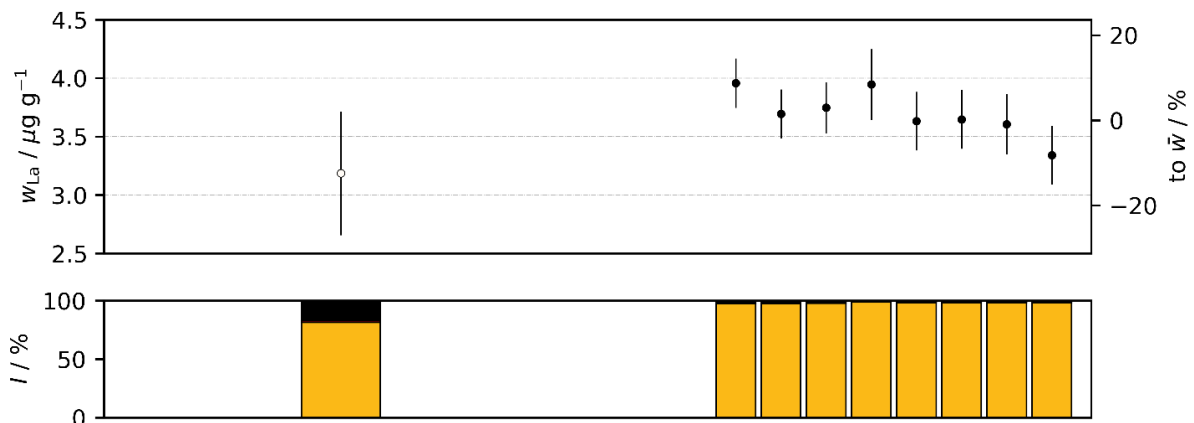


Figure 7: La mass fractions measured on samples of the LED material. White and black circles display results obtained with k_0 -NAA and relative-NAA, respectively; error bars indicate expanded uncertainty ($k = 2$). The bar chart at the bottom reports the contributions to the stated uncertainty for the corresponding value: the highlighted macro-contributors are counting statistics (yellow), efficiency (red) and the remaining ones (black).

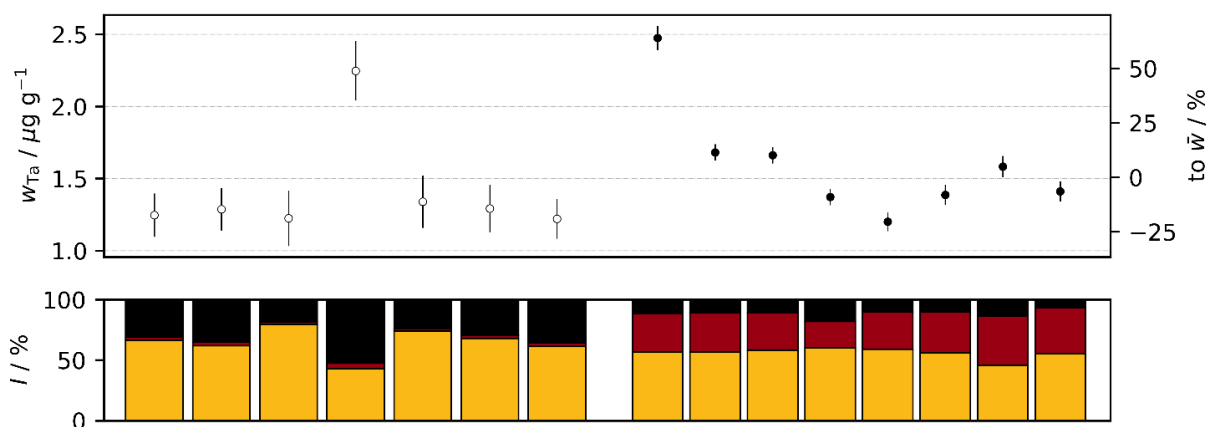


Figure 8: Ta mass fractions measured on samples of the LED material. White and black circles display results obtained with k_0 -NAA and relative-NAA, respectively; error bars indicate expanded uncertainty ($k = 2$). The bar chart at the bottom reports the contributions to the stated uncertainty for the corresponding value: the highlighted macro-contributors are counting statistics (yellow), efficiency (red) and the remaining ones (black).

Data reported in Figure 1-Figure 4 display an overall agreement between results obtained with k_0 and relative methods. Non-homogeneities can better be appreciated from the less uncertain relative method data, but the variability, as denoted by the standard deviation, is within few percent.

4.2. Light Emitting Diodes (LED)

Mass fraction results concerning the quantification of Au, Co, La and Ta in the LED candidate material are hereafter reported; graphics maintain the same information of those related to PCB material shown previously.

Data reported in Figure 5-Figure 8 display a much more noticeable scattering of results especially for what concerns elements found at ppm level.

5. SUMMARY

Analysis on PCB and LED materials recovered from WEEE was performed with relative- and k_0 -standardization methods of INAA technique in order to evaluate the suitability of these materials as a candidate WEEE CRM for Au, Co, La and Ta. The results did not show the presence of noticeable biases between the two standardization methods and confirmed that the measured PCB and LED materials are fit for purpose for the certification of Au, Co and La. For what concerns Ta, unacceptable non-homogeneities were highlighted in LED while La can be certified in PCB. Further studies will involve comparison with SI-traceable techniques based on completely different measurement principles for a broader consensus on the mass fraction values.

6. ACKNOWLEDGEMENTS

This project (20IND01 MetroCycleEU) has received funding from the EMPIR programme co-

financed by the Participating States from the European Union's Horizon 2020 research and innovation programme.

7. REFERENCES

- [1] E. Witkowska, K. Szczepaniak, M. Biziuk, Some applications of neutron activation analysis, *Journal of Radioanalytical and Nuclear Chemistry*, vol. 265, pp. 141-150, 2005. DOI: [10.1007/s10967-005-0799-1](https://doi.org/10.1007/s10967-005-0799-1)
- [2] R. R. Greenberg, P. Bode, E. N. Fernandes, Neutron activation analysis: A primary method of measurement, *Spectrochimica Acta Part B: Atomic Spectroscopy*, vol. 66, pp. 193-241, 2011 DOI: [10.1016/j.sab.2010.12.011](https://doi.org/10.1016/j.sab.2010.12.011)
- [3] F. De Corte, The standardization of standardless NAA, *Journal of Radioanalytical and Nuclear Chemistry*, vol. 248, pp. 13-20, 2001. DOI: [10.1023/a:1010601403010](https://doi.org/10.1023/a:1010601403010)
- [4] M. Di Luzio, M. Oddone, G. D'Agostino, Developments of the k_0 -NAA measurement model implemented in k_0 -INRIM software, *Journal of Radioanalytical and Nuclear Chemistry*, vol 331, pp. 4251-4258, 2022. DOI: [10.1007/s10967-022-08476-x](https://doi.org/10.1007/s10967-022-08476-x)
- [5] M. Blaauw, G. D'Agostino, M. Di Luzio, H. Manh Dung, R. Jacimovic, M. da Silva Dias, R. Semmler, R. van Sluijs, N. Pessoa Barradas, "The 2021 IAEA software intercomparison for k_0 -INAA", *Journal of Radioanalytical and Nuclear Chemistry*, vol 332, pp. 3387-3400, 2023. DOI: [10.1007/s10967-022-08626-1](https://doi.org/10.1007/s10967-022-08626-1)
- [6] k_0 -International Scientific Committee, database of recommended k_0 -data, released August 24, 2020. http://www.kayzero.com/k0naa/k0naaorg/NuclearData_SC/Entries/2020/8/24_Update_of_k0-database_I-128.html.